Appl. Phys. B 58, 273–281 (1994)

Applied Physics B Lasers and Optics

Investigation and Spectral Analysis of the Plasma-Induced Ablation Mechanism of Dental Hydroxyapatite

M.H. Niemz

Department of Applied Physics, University of Heidelberg, Albert-Ueberle-Strasse 3-5, D-69120 Heidelberg, Germany
(Fax: +49 6221/569262, e-mail: bm5@vm.urz.uni-heidelberg.de)

Received 29 September 1993 / Accepted 17 January 1994

Abstract. Experiments on the ablation of dental substance performed with picosecond laser pulses are reported for the first time. A mode locked Nd:YLF oscillator laser was used to generate 25 ps pulses at a wavelength of 1.053 μm. These were seeded and amplified to pulse energies up to 1 mJ in a regenerative amplifier laser at repetition rates up to 1 kHz. Very precise cavities were ablated in the enamel of extracted human teeth by mounting the probes onto a computer controlled 3D translation stage. Scanning electron microscopy and dye penetration tests were performed thereafter. In contrast to longer pulse durations, picosecond pulses ablate with no signs of thermal damage, if the laser pulses are spatially distributed over the target. Definitions of the physical mechanisms "plasma-induced ablation" and "photodisruption" are given. Furthermore, the generated plasma spark has been spectroscopically analyzed. Excitations of calcium and sodium have been observed. From the spectra, the plasma temperature and free electron density could be estimated. By converting part of the laser energy into the second harmonic using a $LiNbO_3$ crystal, a reference amplitude was achieved for the spectra. With this reference signal, a clear distinction could be made between spectra obtained from healthy and caries infected teeth, thus enabling a better control of caries removal in the near future.

PACS: 87.50.Hj, 87.90.+y, 42.55.Rz

The present study deals with the interaction of laser light with solids, in this case dental hydroxyapatite with the chemical formula $Ca_{10}(PO_4)_6(OH)_2$. It is known that optical breakdown in matter can be generated by using ultrashort laser pulses [1]. The physical effects associated with optical breakdown are plasma formation, acoustic shock wave generation and cavitation [2–5]. Time-resolved measurements of the plasma and the shock wave have been made recently [6, 7]. Generally spoken, the initiation of the breakdown process is attributed to electron avalanche ionization [8]. It is the main mechanism responsible for the breakdown in liquids as well as in solids [9]. However, not all relevant physical parameters of this ablation process have been evaluated so far. Especially, the dependence of the ablation threshold on the laser pulse duration is not clearly understood in theory [10]. Also, hydroxyapatite and glass seem to show different shock wave effects, as discussed in this paper.

Since the beginning of laser development several attempts have been made to apply this tool for certain procedures in dentistry, especially in caries therapy. Caries develops when lack of oral hygiene encourages microorganisms to form lactic and acetic acid which dissolve hydroxyapatite. This demineralization process softens the outer shell of the tooth, called enamel, and sometimes even destroys the inner lying dentine and the sensitive pulp chamber. The major aim of using lasers in dentistry is to replace or support conventional drilling machines by lasers in order to achieve a more accurate and painless treatment of caries. Since pain is usually caused by vibration and heat due to friction, it can be avoided by using a contactless operating laser that is working in the "cold" ablation range. Usually cw lasers and pulsed lasers with pulse durations down to the microsecond range generate much heat during the ablation process. This is due to the fact, that in this time frame heat diffusion plays a very important role in the interaction mechanism, which is therefore called thermal interaction [11]. The first lasers used in dentistry, the Ruby laser [12, 13] and the CO_2 laser [14, 15], are representatives of this group. They show very strong thermal side effects, since the temperature increase in the inner tooth reaches values higher than 10°C, thereby injuring the tooth nerves irreversibly.

Meanwhile several experiments have been performed using alternative laser systems. Among these are the Er:YAG laser [16–18] and excimer lasers, especially the ArF laser [19]. The wavelength of the Er:YAG laser at 2.94 μm matches the resonance frequency of the vibrational oscillations of water molecules contained in the teeth, thereby enhancing the absorption of Er:YAG radiation drastically. The absorption is leading to small microexplosions breaking the hydroxyapatite structure. So far, only free-running Er:YAG lasers with pulse durations in the microsecond range have been investigated due to the difficulty in mode locking this laser type with a sufficient energy output. The coinci-

dence of thermal and mechanical ablation effects has led to the term "thermomechanical" interaction [20]. However, microcracks up to 300 μm deep are induced by this type of interaction, that can easily be the origin for new caries development.

The ArF laser at a wavelength of 193 nm shows only very little thermal side effects. Therefore, heat induced ruptures are reduced due to the shorter pulse duration of typically 15 ns. However, the ablation rate, i.e. the ablated volume per pulse, is very low [21]. This ineffectiveness and the general risks of UV radiation are the major disadvantages concerning its use in dentistry, although it may be of importance for other medical applications.

In this study, the ablation of dental substances using picosecond laser pulses is investigated for the first time to my knowledge. The major advantage of applying such short pulse durations is the fact, that the energy threshold for ablating biological tissue scales approximately with the square root of the pulse duration [10, 22]. Hence, lower energies can be used, thereby reducing undesired thermal and mechanical side effects. If the ablation mechanism is governed by a localized plasma formation, it is called "plasma-mediated ablation" or "plasma-induced ablation" [22, 23]. It should be distinguished from "photodisruption", if the ionizing effect of the plasma contributes more to the ablation process than the generated acoustic shock wave. On the other hand, if the ablation is determined by the mechanical rupture of target fragments due to an induced pressure gradient, then the term "photodisruption" is applicable.

The diagnosis of caries by emission spectroscopy has first been proposed by Frentzen et al. [24], but so far only the fluorescence light generated when exposing teeth to UV radiation was examined. Besides, no reference signal was used, which is necessary in order to compare different spectra. In the present paper, a laser-induced plasma at the tooth surface has been spectroscopically analyzed for the first time. Its spectrum depends on the chemical composition of the ionized material. Due to the demineralization process in caries infected teeth, less intensity is expected for the calcium and sodium lines compared to healthy teeth. The results verify this theory and lead to the conclusion, that the Nd:YLF picosecond laser can be used both for diagnosis and therapy of caries.

1. Experimental Setup

1.1. Nd:YLF Picosecond Laser

All experiments were performed using a short pulse, low energy, high repetition rate Nd:YLF laser system. It was designed as a two stage oscillator/regenerative amplifier combination to provide laser pulses with durations down to 30 ps and energies up to 1 mJ at a wavelength of 1053 nm [10]. The overall system is shown in Fig. 1. The HR coated oscillator Nd:YLF rod is pumped by a temperature tuned Spectra Diode Labs 1 Watt Diode Laser (DL) using beam shaping and Collimating Optics (CO). An Acoustooptic Mode Locker (AOM) is placed near the flat 10% Output Coupler (OC). For active amplitude modulation an amplified 80 MHz rf signal is applied to this device, generating a train of short laser pulses with typical durations of 25 ps each (Fig. 2). A realtime autocorrelation system allows continuous supervision of the pulse width. For the purpose of selecting the 1053 nm transition, a Brewster plate Polarizer (BP) was added to the cavity.

At the Half-Wave Plate (HWP) the 160 MHz pulse train, consisting of 0.2 nJ pulses, experiences a 90° rotation of the polarization vector. Using a 4% reflecting Mirror (M3) and a polarizing beam splitter, the oscillator pulses are then injected into the regenerative amplifier unit [25]. The 76 mm amplifier Nd:YLF rod is pumped by a single flashlamp, controlled by a standard Quantronix 204A power supply. The cavity employs two highly reflecting mirrors with a radius of curvature of 1 m each. Applying a 2 kV voltage signal with up to 1 kHz repetition rate to a $LiNbO_3$ Pockels Cell (PC) provides half-wave retardation per round-trip. In combination with the double-pass half-wave retardation of the intracavity Quarter-Wave Plate (QWP), a selected oscillator pulse is seeded and trapped in the amplifier unit. The driving of the Pockels cell is synchronized to the mode locking process by feeding the 80 MHz rf signal into a special divider and timer logic. After about 100 roundtrips in the cavity the seeded pulse reaches its saturation limit. The pulse energy can be boosted up to 1 mJ, corresponding to an amplification of 10^6 of the oscillator output energy. Installation of an Aperture (A) restricts the laser operation to the fundamental TEM_{00} mode. At maximum gain the Pockels cell driver switches back to 0 V, causing no retardation. The polarization vector is now rotated by 90° as the pulse double-passes the quarter-wave plate and the Pockels cell in the left part of the cavity. Consequently, the amplified pulse is then reflected at the polarizing beam splitter and dumped out of the regenerative amplifier. Mirror M3 is now transmitting 96% of the amplified pulse energy. Using Mirror M4, the pulse train is finally injected into the application unit. Autocorrelation of these pulses showed, that their pulse duration has slightly increased to about 30 ps due to dispersion inside the amplifier cavity.

Nd:YLF is a solid-state optical gain medium closely related to Nd:YAG, but without several of its undesirable features. Unlike Nd:YAG, it is only weakly affected by thermal birefringence [26]. This characteristic allows a simpler cavity design and a higher ratio of TEM_{00} to multimode average power [27]. Nd:YLF also has a longer upper-level fluorescence lifetime compared to Nd:YAG, which enables greater energy storage and thus higher peak pulse powers under Q-switched or mode-locked operation.

1.2. Application Unit

For the sake of automating the tissue experiments, an application unit was also developed. This device consists basically of delivering optics and a computer controlled three-axes translation stage. After expanding the laser beam four times by the Lenses L2 and L3, it was focussed tightly onto the tissue sample by the Lens L4. The focus spot was measured by the knife edge method and had a diameter of about 30 μm. Stepping motors connected to the translation stage allow precise spot-to-spot movements of the tooth within 1 μm. A software package gives the user a choice of

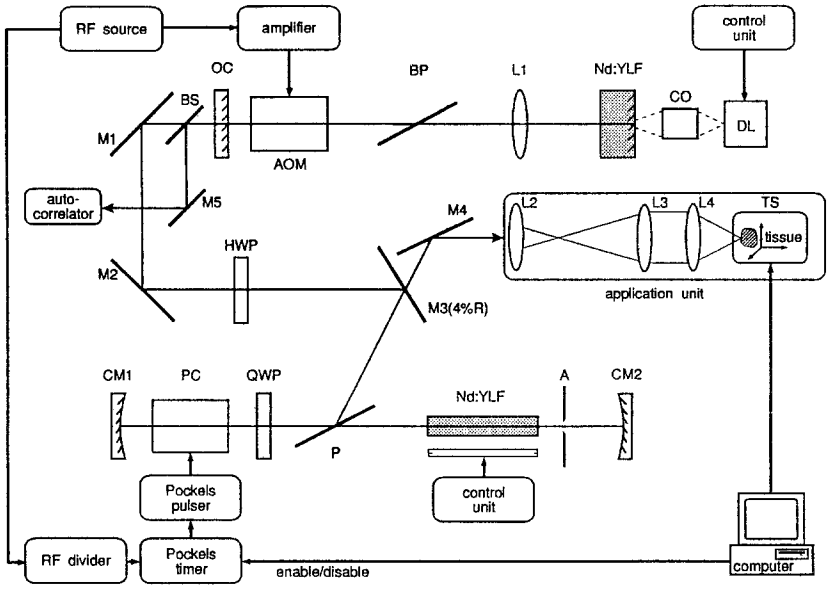

Fig. 1. The picosecond Nd:YLF laser system

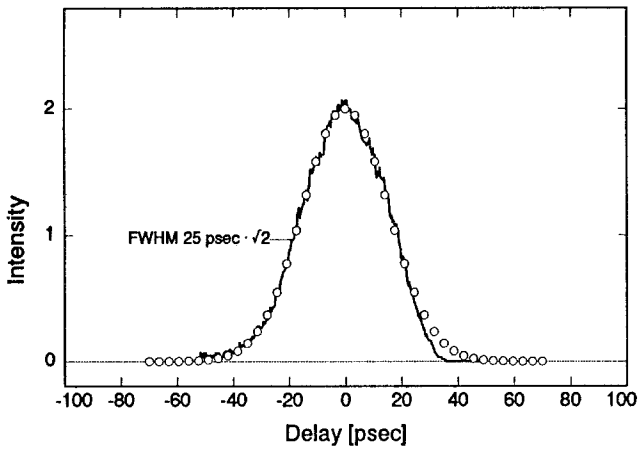

Fig. 2. Autocorrelation trace of 25 ps laser pulses generated in the Nd:YLF oscillator

different ablation patterns. Mainly, square and circular geometries have been used in the experiments presented. The motor control software also has the capability of disabling the dumping mechanism of the Nd:YLF laser amplifier, thus providing exact single-shot operation with this laser system.

1.3. Spectroscopy

For the purpose of spectroscopically analyzing the generated plasma spark, the spark was optically imaged onto the entrance pupil of a spectrometer using a lens with 50 mm focal length. Before the experiments, this lens was adjusted using a HeNe laser illuminating the spark backwards through the spectrometer. A spectrometer with an optical diffraction grating was used (ISA Instruments model 640-HR). The angle of the grating was controlled by a stepping motor. The signal was detected by a photomultiplier and submitted onto a fast programmable digitizer (Tektronix model 7912AD). From there the data were fed into a computer and processed. The spectra were scanned with a resolution of typically 0.2 nm. For single lines, the sampling distance of the wavelength was 0.25 Å per step. During the experiment the tooth was moved within the focal plane of the cutting lens to ensure equivalent surface conditions. To account for slight deviations of the signal amplitude at the same wavelength, each measurement was repeated five times.

A BBO crystal was used to externally generate the second harmonic of the laser wavelength. This non-linear crystal was cut at an angle of 22.8° to the optical axis (type-I phase matching) and positioned between Mirror M4 and Lens L2. It was adjusted in a way, that about 10 μJ of the pulse energy were converted to the second harmonic. By mixing it with the fundamental wavelength, the normalization of the spectra was facilitated: The diffuse reflection of the second harmonic at the tooth surface was also detected by the photomultiplier and used as a reference signal.

1.4. Tooth Preparation

The teeth used for this study were extracted human sound molars obtained from the Dental Policlinic, Heidelberg. For better handling, their roots were embedded in a 1 cm^3 plastic cube. They were always kept in humid environment to avoid artifical cracking due to dryness. All laser ablations were performed inside the enamel of the tooth. This outer shell contains 95% (by weight) hydroxyapatite, 4% water and 1% organic matter. Artificial white caries lesions were prepared by the Dental Policlinic using synthetic saliva buffered at pH 4.8 with acetic acid.

After the experiments the teeth were dried in the vacuum chamber of an exsiccator and coated with a 30-nm-thick gold layer. The morphologic changes induced by the laser radiation were studied using a scanning electron microscope (Amray 1810). For accurate measurements of the ablation

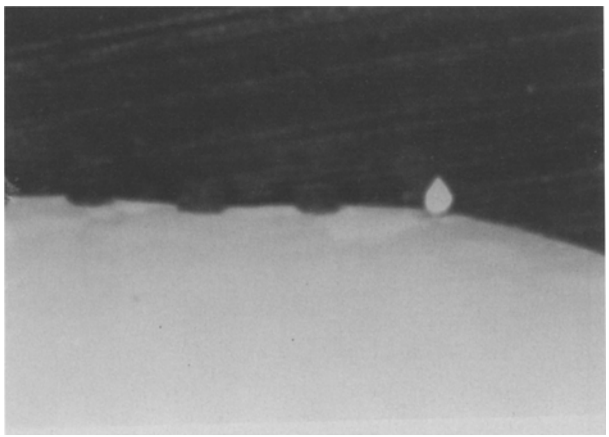

Fig. 3. Plasma spark at the tooth surface. The width of the plasma is about 30 μm (total magnification: 300 ×)

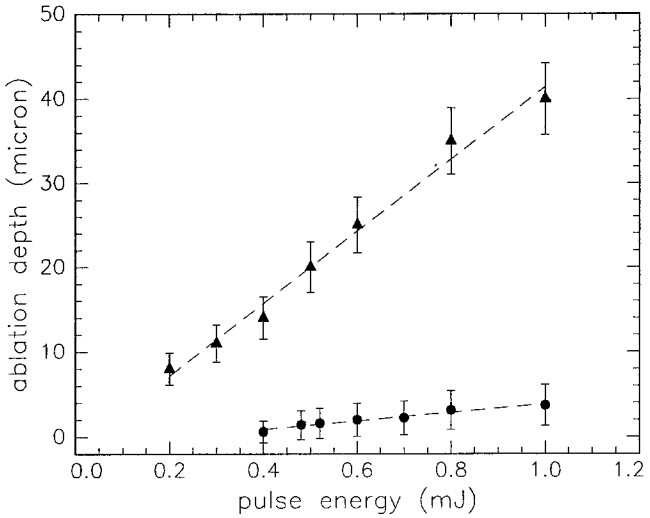

Fig. 4. Ablation curves of healthy (•) and carious (▲) enamel for 30 ps laser pulses at a focal spot size of 30 μm

depth, the samples were cut into 500-μm-thick slices using a diamond saw microtome.

For temperature measurements during laser exposition the pulp chamber inside the tooth was excavated by a preparation diamond and filled with heat conducting paste. The temperature was measured with an inserted thermocoupler.

In order to investigate the effect of the shock wave, dye penetration tests were performed. For these tests the samples were prepared the same way, except that they were exposed for two hours to 1% neofuchsine staining solution immediately after the laser experiment. The penetration of the stain into the surrounding enamel could then be observed at the slices using a light microscope. Also, in different experiments, microscope glass plates were used as targets to study shock wave effects. They were examined afterwards by scanning electron microscopy.

2. Results and Discussion

With a pulse energy of 1 mJ, a pulse duration of 30 ps and a focal spot size of 30 μm, the power density at the focus reaches values $> 10^{12}$ W/cm^2. Hence, the amplitude of the electric field exceeds 10^7 V/cm, thereby initiating an optical breakdown. A microplasma is generated, ionizing the material at the focal point. The absorption of succeeding laser radiation is strongly enhanced by the plasma [23]. Therefore, all interaction effects are mainly localized at the surface of the target. A picture of the plasma spark at the tooth surface is shown in Fig. 3. In this case the pulse energy was set to 500 μJ. The photograph was taken with a high optical magnification setup using a 200 mm zoom lens. Adjacent to the spark three ablated holes are visible. The total magnification of the picture is 300×. The width of these holes and the extension of the plasma spark are both on the order of 30 μm, given by the focal spot size. The spark is generated at the tooth surface and extends into air in front of it.

In Fig. 4 the ablation curves (ablation depth per pulse versus pulse energy) of healthy and carious enamel are shown. In case of healthy enamel, plasma sparking was already visible at about 200 μJ. With the focal spot size of 30 μm, the ablation threshold can then be determined to be about 30 J/cm^2. For carious enamel, plasma generation started at about 100 μJ. Its ablation threshold is therefore about 15 J/cm^2. These ablation thresholds are slightly higher compared to other tissues [23]. In the investigated range of pulse energies, both curves are mainly linear. Linear regression analysis yields, that the slopes in Fig. 4 are about 1 μm/200 μJ and 9 μm/200 μJ, respectively. The removal of carious substance with this laser is therefore about ten times more efficient. The achievable ablation depth per pulse at moderate pulse energies is smaller than observed with the Er:YAG laser [17]. However, taking the high repetition rate of the Nd:YLF laser system into account, its effectiveness should be sufficient for dental applications.

Figures 5a,b show Scanning Electron Micrographs (SEM) of tetragonal cavities produced with the Nd:YLF picosecond laser. Figure 5a represents a cavity ablated in healthy enamel, whereas Fig. 5b shows a cavity within artificial caries. Both cavities have lateral dimensions of 1 mm×1 mm and a depth of about 400 μm. They were created by distributing 1 mJ laser pulses onto 40 lines over the tooth surface with 400 lasered spots per line, and repeating this procedure ten times for the cavity in Fig. 5a and once for the cavity in Fig. 5b. Thus, a total number of 160 000 laser shots was necessary for the cavity in healthy enamel and only one tenth of this number was needed to generate the cavity in carious enamel. This indicates again, that the ablation rate of demineralized substance is about ten times higher than for intact enamel. Taking the focal spot size into account, each spot of the ablated area was irradiated approximately 100 times in Fig. 5a (overlay of ten shots during one line multiplied by ten procedures) and ten times in Fig. 5b. Therefore, the ablation depth per pulse is about 4 μm for healthy enamel and about 40 μm for carious enamel, as already shown in Fig. 4. The bottom surface of the cavity in healthy enamel (Fig. 5a) is slightly rougher than the surface in carious enamel (Fig. 5b). This is not a disadvantage, because rougher surfaces facilitate the adhesion of

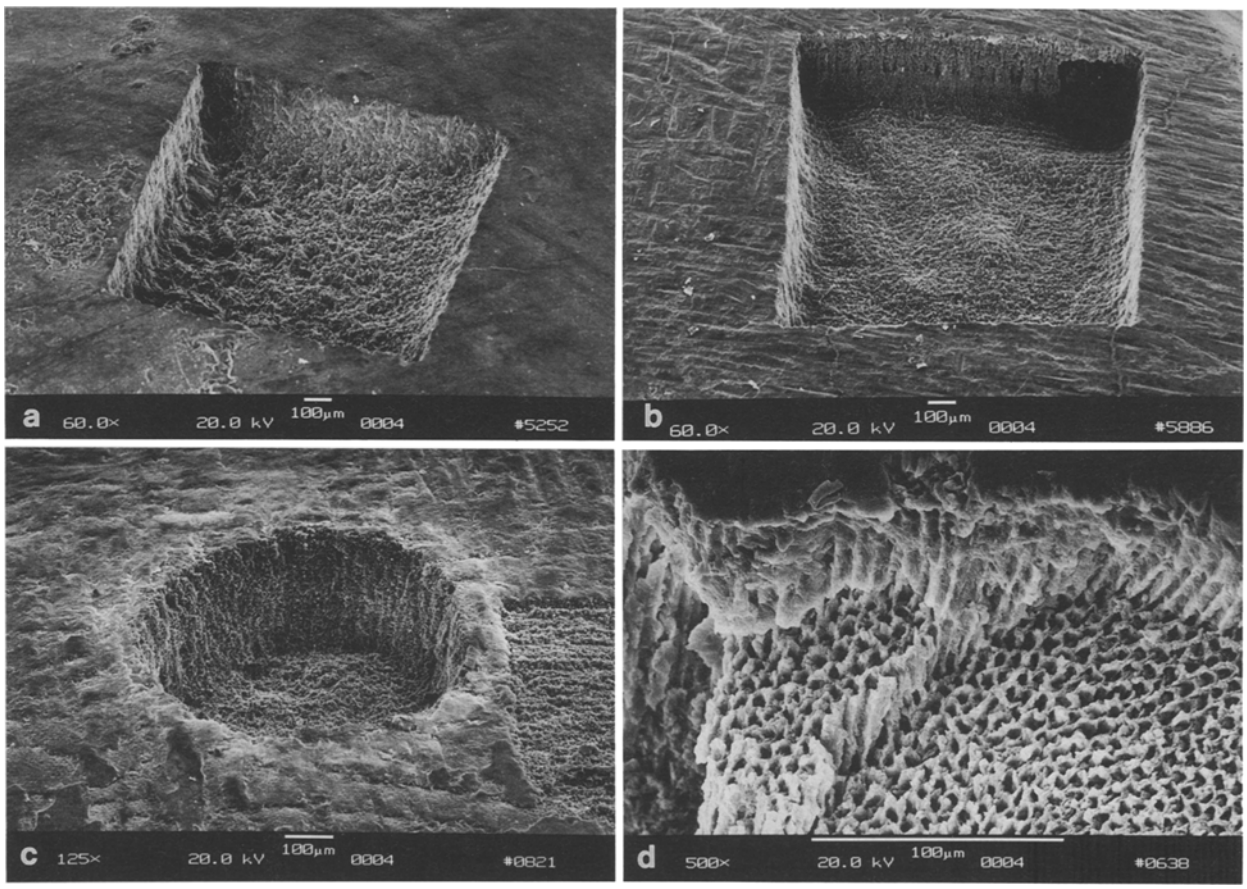

Fig. 5. a SEM of a cavity inside healthy enamel generated by 160 000 laser pulses, distributed among 100 pulses per spot (pulse energy: 1 mJ). **b** SEM of a cavity inside carious enamel generated by 16 000 laser pulses, distributed among ten pulses per spot (pulse energy: 1 mJ). **c** SEM of a cavity inside carious enamel generated by 6000 laser pulses, distributed among twenty pulses per spot (pulse energy: 400 μJ). **d** Enlargement of a carious region partly ablated by the Nd:YLF laser

filling materials in dental practice. Both cavities have a very precise geometry and especially the edges are very clean and sharp.

A different geometry for ablating carious enamel is shown in Fig. 5c. In this case, the tooth on the translation stage was moved in a way, that a circular ablation area was obtained. The cylindrical cavity has a diameter of 500 μm and a depth of about 300 μm. 6000 laser pulses at a pulse energy of 400 μJ each were applied. Taking the spatial overlap of the pulses into account, each spot of the ablated area was irradiated by approximately twenty pulses. The ablation depth per pulse is therefore on the order of 15 μm, which is in agreement with the ablation depths shown in Fig. 4. The cylindrical shape of the cavity is very precise and comparable to the quality achieved by mechanical drills. Figure 5d shows an enlargement of a tooth, in which part of a carious region has been removed by the Nd:YLF laser. The unexposed surface is located at the top of the picture. Caries infected areas can easily be recognized by hollow columns of hydroxyapatite, due to the demineralization process.

Figure 6a illustrates the effect that occurs, when focussing 1000 laser pulses onto the same spot on the tooth at a repetition rate of 1 kHz. Within a distance of about 100 μm from the application site a zone of melted substance can be seen. Deep and long thermal cracks are found in the periphery arranged radially to the laser impact. These results prove that even picosecond laser pulses can induce thermal damage, if more heat is generated than diffused per unit time during a multiple overlap of consecutive pulses. Recrystallization in form of plasma sublimations was also found (Fig. 6b). The cubic crystal structure differs from the original microscopic structure of enamel. For a better understanding of this result, it is important to know, that the enamel of the tooth originally consists of little hydroxyapatite fragments embedded into an organic matrix. Since the organic material is evaporated in the laser plasma, hydroxyapatite can afterwards crystallize in its natural form. Analysis of back-scattered electrons in the electron microscope proved, that the sublimations consist of the same chemical compounds as the original hydroxyapatite.

With the thermocoupler the temperature inside the pulp chamber of the tooth was measured during the experiments. A temperature increase of up to 8°C was observed when focussing the laser beam always onto the same spot at a repetition rate of 1 kHz. On the other hand, the temperature increase was negligible when moving the tooth between individual laser pulses. The interaction mechanism is even then basically non-thermal, if the spatial overlap of consecutive pulses is only partially reduced, as demonstrated with the cavities shown in Figs. 5a,b.

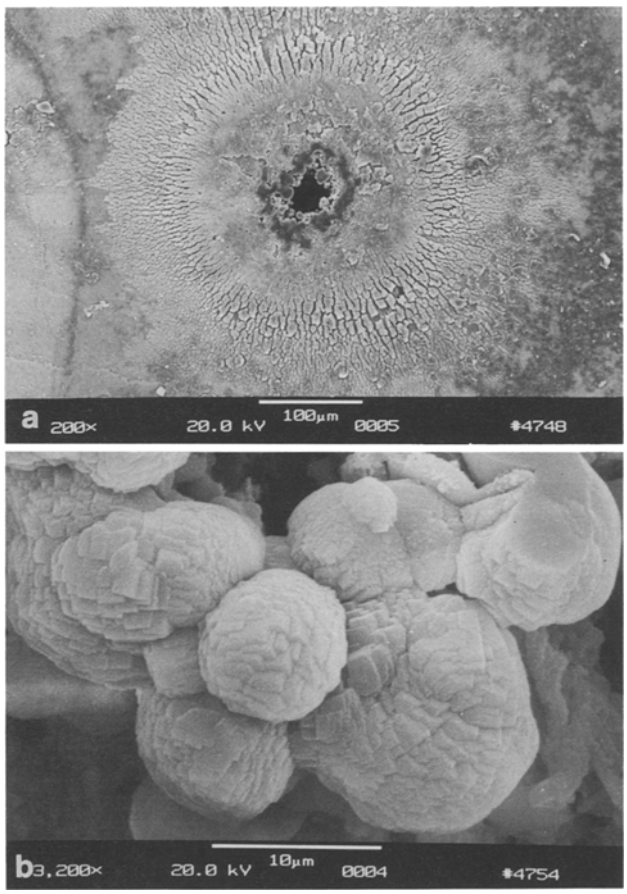

Fig. 6. a Hole in tooth created by 1000 laser pulses at a repetition rate of 1 kHz without scanning the beam. **b** Enlargement showing recrystallization in form of plasma sublimations

In Figs. 7a–c three spectra of the plasma spark are given. In these experiments, the laser pulse energy was set to 500 μJ. Figure 7a shows the spectrum of a healthy tooth, while Figs. 7b,c were obtained from two different regions of a caries-infected tooth. Calcium in neutral and singly ionized states and the major doublet of neutral sodium can be found in all spectra according to listed emission wavelengths [28]. They are the most occuring minerals in teeth. Phosphorus was also expected, but neither of its strongest emission lines at 602.4 nm and 603.4 nm were observed. The two lines between 390 nm and 400 nm probably result from neutral calcium (394.8 nm, 397.3 nm) and the major emission of singly ionized calcium (393.3 nm, 396.8 nm). One strong peak can be seen at about 526.5 nm, that arises partly from a multiplet of calcium lines and from the external Second-Harmonic Generation (SHG). Therefore, in the spectra, it is labeled with "Ca & 2ω". SHG at the tooth surface is also conceivable, but its amplitude is expected to be surpassed by the calcium multiplet. The detected signal at 526.5 nm was normalized to unity. This normalization is useful, when comparing spectra of healthy and carious teeth as seen in Figs. 7a–c. The spectra of the caries-infected teeth show a strong amplitude decrease for all mineral lines due to the demineralization process induced by caries. Slight deviations in the ratio of calcium and sodium intensities were observed due to different demineralization stages of caries.

The normalization realized in this study is only correct, if the diffuse reflectivities of healthy and carious teeth are the same for the second harmonic at 526.5 nm. This was tested by filtering out the fundamental wavelength, thereby preventing plasma generation, and measuring the reflected signal while moving different areas of the tooth through the focus. No significant difference in the intensities was observed. However, since the intensities of the calcium multiplet at 526.5 nm are also decreased in carious teeth, the ratio of SHG photons contributing to the normalization signal at 526.5 nm varies. Therefore, a direct comparison of absolute intensities cannot be derived from these spectra. In order to achieve this aim, a different wavelength could be used for normalization (e.g. 632.8 nm of a HeNe laser).

An exact evaluation of the plasma temperature is difficult due to the short life time of the plasma. Temporal measurements are required to understand the dynamical behaviour of the plasma temperature and the free electron density. However, by comparing the intensities of two different calcium lines, an estimate of a mean plasma temperature can be given. According to [29], the following relation is valid for two spectral lines of the same atomic species in the same ionization stage

$$\frac{I_1}{I_2} = \frac{A_1 g_1 \lambda_2}{A_2 g_2 \lambda_1} \exp\left(-\frac{E_1 - E_2}{kT}\right), \tag{1}$$

with I = intensity, A = transition probability, g = statistical weight of the upper energy level, λ = wavelength, E = upper energy level, k = Boltzmann constant, and T = plasma temperature. Differentiating (1), one obtains:

$$\frac{\Delta T}{T} = \frac{kT}{E_1 - E_2} \frac{\Delta(I_1/I_2)}{I_1/I_2} . \tag{2}$$

Hence, the accuracy of the temperature determination can be improved by choosing two upper energy levels, that are far apart from each other. The accuracy of the measured intensities is the best for singlets. Because of these two reasons, the intensities at the two calcium wavelengths λ_1 = 422.7 nm and λ_2 = 585.7 nm were compared. According to [28], the parameters in (1) are then as follows:

$$A_1 = 2.18\,10^8\,\mathrm{s}^{-1}\,, \quad A_2 = 0.66\,10^8\,\mathrm{s}^{-1}\,, \quad g_1 = 3\,, \quad g_2 = 5\,,$$
$$E_1 = 2.94\,\mathrm{eV} \quad \text{and} \quad E_2 = 5.05\,\mathrm{eV}\,.$$

On the average, the measured intensity ratio was about: $I_1/I_2 \approx 4$. Therefore, the mean temperature in (1) can be calculated to be about 5.6 eV.

Figures 8a,b show spectra of a different series of experiments. Again, a clear distinction can be made between healthy and carious regions of the tooth. These spectra were obtained at a pulse energy of 300 μJ. In this case, the ratio of the intensities at the wavelengths 422.7 nm and 585.7 nm was about: $I_1/I_2 \approx 5$. This corresponds to a slightly lower plasma temperature of about 3.5 eV due to a lower pulse energy.

In order to evaluate the free electron density of the plasma, the spectral width of the calcium singlet at 422.7 nm was measured. No significant dependence of the width on the

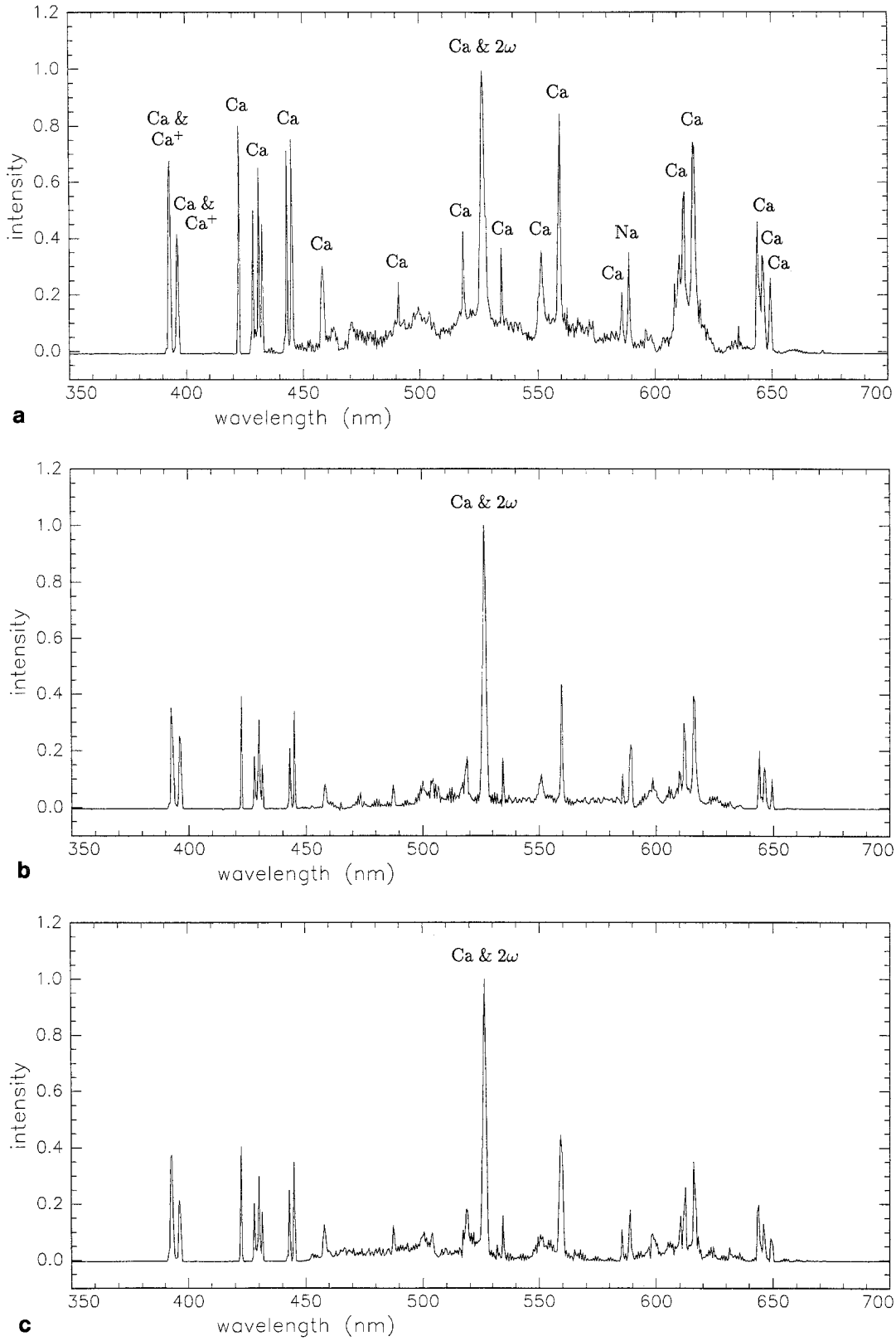

Fig. 7. **a** Spectrum of healthy enamel (pulse energy: 500 μJ). **b** Spectrum of caries infected enamel (pulse energy: 500 μJ). **c** Spectrum of caries infected enamel (pulse energy: 500 μJ)

pulse energy was observed. The measured width (HWFM) was about 1.5 Å. Using the plasma temperatures obtained above and listed values of emission widths [30], the electron density can then be estimated to be about $10^{18}\,\mathrm{cm}^{-3}$.

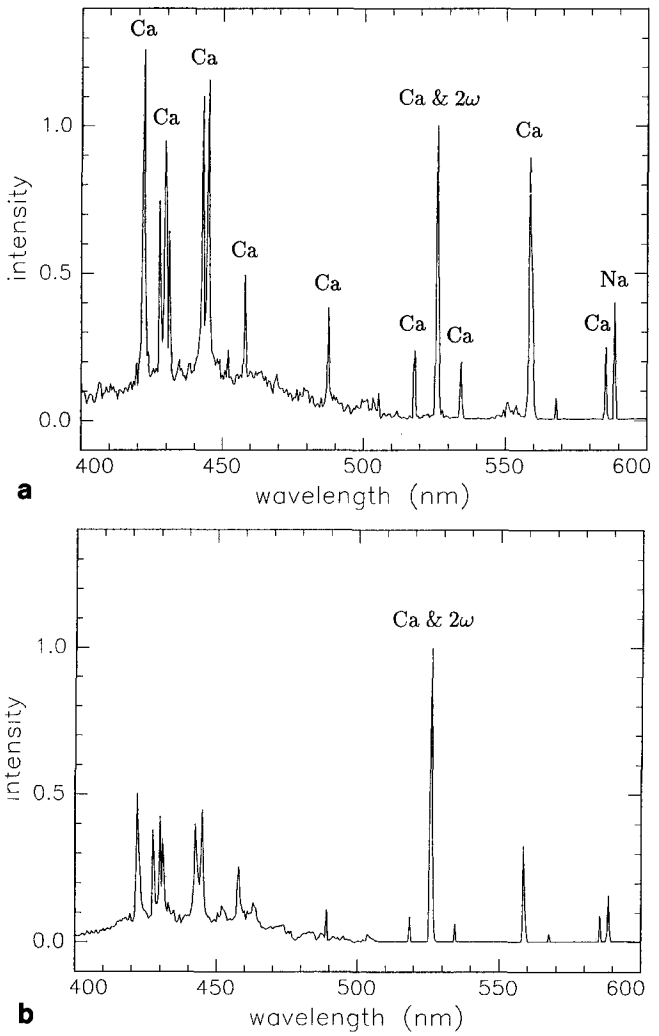

Fig. 8. **a** Spectrum of healthy enamel (pulse energy: 300 μJ). **b** Spectrum of caries infected enamel (pulse energy: 300 μJ)

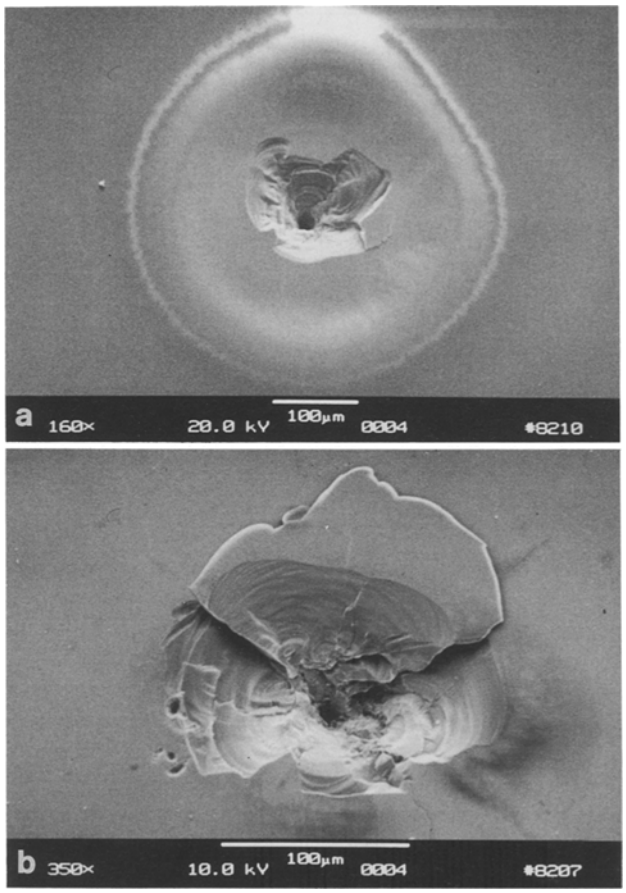

Fig. 9. **a** SEM of a glass plate irradiated by ten laser pulses at the beam focus (pulse energy: 1 mJ). The anterior surface pointing to the laser source is shown. **b** SEM of a glass plate irradiated by ten laser pulses at the beam focus (pulse energy: 1 mJ). The posterior surface is shown

The results of the dye penetration tests showed that microcracks induced by the Nd:YLF laser do not exceed 20 μm. This depth is comparable to cracks induced by conventional drilling machines. However, the dye penetration in samples exposed to Er:YAG or Ho:YAG laser radiation was found to be one to two orders of magnitude deeper [31]. In such fissures new caries could easily develop. The dye penetration tests for the Nd:YLF laser pulses suggest, that shock wave effects inside the enamel are negligible at moderate pulse energies.

In Figs. 9a,b the effect of the shock wave on a 90 μm thick microscope glass plate is shown. The photographs show the anterior and posterior side, respectively, viewed from the laser source. In each case, ten laser pulses at an energy of 1 mJ were focussed onto the anterior surface and generated a plasma. Obviously, an acoustic shock wave emerged into the glass and created a typical cone-shaped crater. Hence, in glass, the shock wave is primarily responsible for the ablation. The concentric ring around the crater might give an estimate of the spatial interaction zone of the glass with the shock wave. These pictures prove that the impact of the shock wave is completely different for enamel and glass. This behaviour probably has its origin in the microscopic structure of both materials. Since the hydroxyapatite inside the enamel is embedded into an organic matrix, an intruding shock wave is strongly damped and cannot cause major ruptures. On the other hand, glass easily splinters if exposed to high amplitude acoustic waves. Of course, further studies need to be done to evaluate this phenomenon in detail. Especially, any morphological changes at the junction of enamel and dentine have to be investigated, although preliminary hardness tests measuring the impact of a diamond tip seem to prove that there are none.

The comparison of the ablation results for teeth and glass indicate, that different ablation mechanisms are involved even at the same power density. In both cases, plasma ionization takes place. But the target material determines whether associated shock waves are of primary or only secondary importance. If mechanical ruptures are induced as in glass, the mechanism is characterized by photodisruption. In other cases, i.e. if mechanical side effects are negligible as in teeth, the term "plasma-induced ablation" is more appropriate.

3. Conclusions

The present paper gives a deeper insight into the physical ablation mechanism of matter with picosecond laser pulses. Temperature increases and shock wave phenomena were discussed. The ablation curves of healthy and carious enamel were measured. It has been shown that picosecond pulses interact non-thermally, if the laser beam is scanned over the target. However, thermal effects were induced when applying a 1 kHz pulse train onto the same spot. Shock wave generation has been proved by cone-shaped impacts on glass plates positioned at the laser focus. But dye penetration tests have shown, that this shock wave does not lead to crack formation within the tooth at moderate pulse energies close to the ablation threshold. Therefore, the ablation mechanism of teeth can primarily be attributed to the ionization caused by the plasma. The plasma temperature and the free electron denisty were estimated from plasma emission spectra. It was shown that the picosecond Nd:YLF laser is a viable alternative to other lasers regarding their application in dentistry. Especially selective caries removal is enabled because of two reasons. On the one hand, the ablation rate of caries is higher than of healthy enamel, causing the ablation procedure to slow down, if all caries is removed. On the other hand, the generated plasma spark can be spectroscopically analyzed in real time. By comparing the amplitude at a reference wavelength with any of the mineral lines, a computer-controlled laser system could then possibly decide, whether all caries has been removed or not. With this option the laser could not only be a less painful but also a more precise tool for dental applications, especially when considering how often a tooth may be refilled. In dental practice, usually more material is removed than necessary, just to make sure that all caries is taken away. With such a control as described above, the amount of removed substance could be minimized. For this aim, of course, further investigations need still to be done.

Acknowledgements. The author gratefully acknowledges Dr. T. Pioch at the Dental Clinic of the University Hospital, Heidelberg, for his support in obtaining the tooth samples and the SEMs, and A. Mindermann for her help in measuring the spectra.

References

1. N. Bloembergen: IEEE J. QE-**10**, 375 (1974)
2. M.P. Felix, A.T. Ellis: Appl. Phys. Lett. **19**, 484 (1971)
3. F. Docchio: Appl. Opt. **27**, 3661 (1988)
4. F. Docchio: Appl. Opt. **27**, 3669 (1988)
5. C.E. Bell, J.A. Landt: Appl. Phys. Lett. **10**, 46 (1967)
6. B. Zysset, J.G. Fujimoto, T.F. Deutsch: Appl. Phys. B **48**, 139 (1989)
7. A. Vogel, P. Schweiger, A. Frieser, M.N. Asiyo, R. Birngruber: IEEE J. QE-**26**, 2240 (1990)
8. A.S. Epifanov: IEEE J. QE-**17**, 2018 (1981)
9. C.A. Sacchi: J. Opt. Soc. Am. B **8**, 337 (1991)
10. M.H. Niemz, T.P. Hoppeler, T. Juhasz, J.F. Bille: Lasers Light Ophthalmol. **5**, 149 (1993)
11. J.L. Boulnois: Lasers Med. Sci. **1**, 47 (1986)
12. R.H. Stern, R.F. Sognnaes: J. Dent. Res. **43**, 873 (1964)
13. L. Goldman, P. Hornby, R. Mayer, B. Goldman: Nature **203**, 417 (1964)
14. R.H. Stern, J. Vahl, R.F. Sognnaes: J. Dent. Res. **51**, 455 (1972)
15. J.W. Frame: Br. Dent. J. **158**, 125 (1985)
16. U. Keller, R. Hibst: Dtsch. Zahnärztl. Z. **44**, 600 (1989)
17. R. Hibst, U. Keller: Lasers Surg. Med. **9**, 338 (1989)
18. U. Keller, R. Hibst: Lasers Surg. Med. **9**, 345 (1989)
19. T. Liesenhoff, T. Bende, H. Lenz, T. Seiler: Dtsch. Zahnärztl. Z. **45**, 14 (1990)
20. M. Frentzen, H.J. Koort: Dtsch. Zahnärztl. Z. **46**, 443 (1991)
21. P. Rechmann, T. Hennig, R. Kaufmann: Zahnärztl. Welt **101**, 150 (1992)
22. D. Stern, C.A. Puliafito, E.T. Dobi, W.T. Reidy: Arch. Ophthalmol. **107**, 587 (1989)
23. M.H. Niemz, E.G. Klancnik, J.F. Bille: Lasers Surg. Med. **11**, 426 (1991)
24. M. Frentzen, H.J. Koort, C. Tack: Dtsch. Zahnärztl. Z. **45**, 199 (1990)
25. P. Bado, M. Bouvier, J.S. Coe: Opt. Lett. **12**, 319 (1987)
26. J.E. Murray: IEEE J. QE-**19**, 488 (1983)
27. T.M. Pollak, W.F. Wing, R.J. Gasso, E.P. Chicklis, J.P. Jenssen: IEEE J. QE-**18**, 159 (1982)
28. R.C. Weast (ed.): *Handbook of Chemistry and Physics* (CRC, Boca Raton 1981) Chap. E
29. W. Lochte-Holtgreven: *Plasma Diagnostics* (North-Holland, Amsterdam 1968) p. 181
30. H.R. Griem: *Plasma Spectroscopy* (McGraw-Hill, New York 1964) p. 496
31. M.H. Niemz, L. Eisenmann, T. Pioch: Schweiz. Monatsschr. Zahnmed. **103**, 1252 (1993)